Nonlinear Design Scaling of Electric Machines Based on Hybrid DE and Meta-modeling – Application to Synchronous Motors with Combined PM Stator and Reluctance Rotor Excitation

Oluwaseun A. Badewa
SPARK Lab, Pigman Eng. College
University of Kentucky
Lexington, KY, USA
o.badewa@uky.edu

Dan M. Ionel
SPARK Lab, Pigman Eng. College
University of Kentucky
Lexington, KY, USA
dan.ionel@ieee.org

***Abstract*—This paper presents an innovative method for nonlinear scaling of electric machines by integrating machine learning (ML)-based meta-modeling with a differential evolution (DE) algorithm. The technique is applied to high-performance combined-excitation synchronous electric motors which exhibit highly nonlinear characteristics, making performance scaling challenging. The proposed approach employs an ML meta-model trained on data obtained from finite element analysis (FEA), utilizing an experimentally validated model for nonlinear scaling and performance prediction at different power ratings. The accuracy of the meta-model in capturing the nonlinear relationships between design parameters and motor performance is first assessed using metrics such as R-squared (R^2) and normalized root mean square error (NRMSE) prior to nonlinear scaling. The scaled results are then compared with those obtained from finite element analysis (FEA), demonstrating good correlation within acceptable tolerances. This hybrid ML-DE approach aims to provide a robust and resource-efficient method for electric motor design, optimization, and performance estimation.**

***Index Terms*—Meta-modeling, machine learning, artificial intelligence, differential evolution, finite element analysis, nonlinear scaling, performance estimation, synchronous motor, spoke-type PM, reluctance rotor.**

I. Introduction

Research into performance improvement of electric motors is an ever-growing field owing to the increased electrification, especially of mobility and propulsion, and global efforts to reduce emissions [1]–[5]. Great advancements have been made in using analytical tools such as finite element analysis and modeling to bridge the gap between results obtained from simulation and experimentation [6]–[8]. Therefore, performance prediction of key metrics such as power density, efficiency, and losses can be done with increased accuracy [9].

Due to the inherent nonlinearities typical in electric motors, the computational effort required to obtain these optimal designs with accurate performance predictions is huge, especially considering the different power ratings needed for various applications. Several limited methods of nonlinear performance scaling have therefore been investigated based on, for example, a factor of specific thrust [10], optimal design studies, [11], and studies using scalable models [12] to understand the trends in performance and size.

The stator permanent magnet (PM)-combined excitation synchronous motor topology, which shows highly nonlinear behavior, especially at high current densities, has been proposed for a wide spectrum of applications ranging from kW-level electric motors for EVs to multi-MW applications in wind turbines [13], [14]. This is due to its potential benefits of high power density, fault tolerance, reduced losses, and easy adoption of the latest technology in terms of advanced cooling and hairpin winding using rectangular slots [15]. The design optimization of this topology has been carried out using the well-established multi-objective differential evolution (MODE) employing finite element analysis (FEA) for set objectives and power ratings depending on the proposed application. This approach requires several generations of designs and is typically computationally intensive [7], [14].

More recently, the use of machine learning (ML) and artificial intelligence (AI) has been proposed for the design optimization of electric machines. This is to leverage advancements in big data and large-scale computation [16]–[19]. The resultant meta-model or surrogate models based on, for example, Artificial Neural Networks seek to use reduced amounts of data to accurately predict motor performance, thereby reducing the computational effort needed for optimization [19]–[22]

This paper investigates the application of an ML meta-model to address the challenges of nonlinear scaling of electric machines such as the combined-excitation synchronous motor. The proposed approach offers a robust methodology for such special topology machines, filling a gap in existing literature. The meta-model, trained with finite element analysis (FEA) data obtained through differential evolution (DE) using an experimentally validated FEA model, aims to capture the nonlinearities and complex relationships between performance and geometry across different power ratings. The subsequent sections of this paper include a review of motor topology and

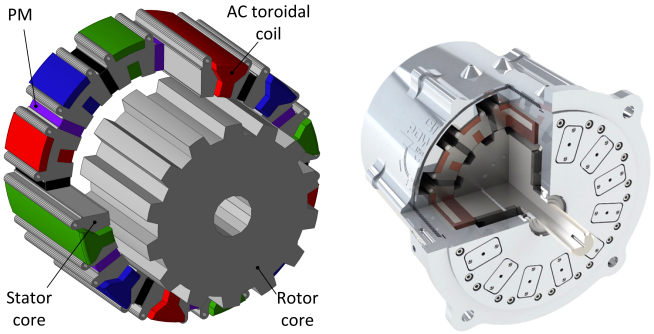

Fig. 1. The investigated combined-excitation synchronous motor topology as a (a) solid model for 3D FEA with labeled parts, (b) 3D CAD model of the constructed prototype.

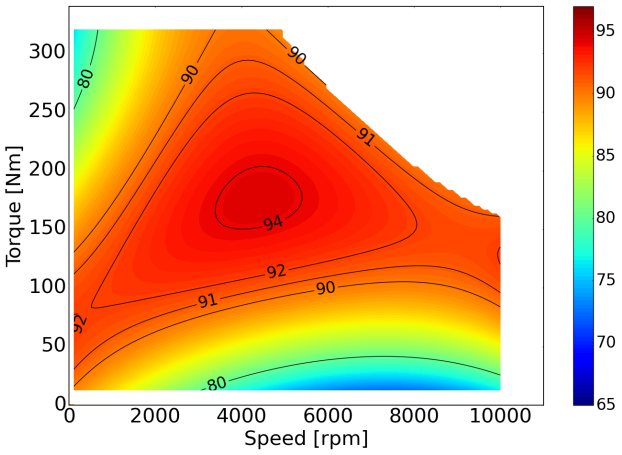

Fig. 2. Measured efficiency map of the prototype machine at high operating temperature showing capability for high-efficiency operation

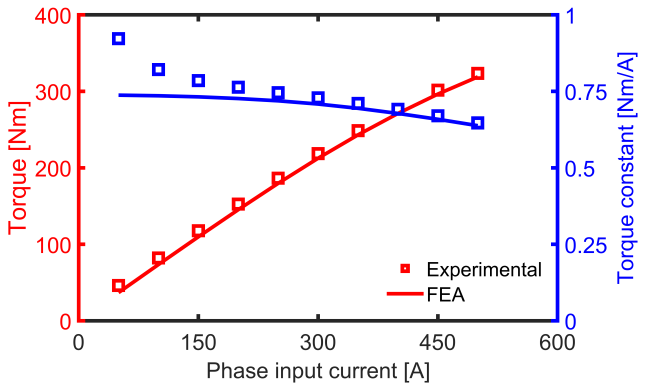

Fig. 3. Comparison of experimental and FEA results for the PM stator-combined excitation motor prototype showing good correlation for the static torque and torque constant with increasing phase currents.

experimental validation, a discussion of the DE/FEA data gathering process, and an outline of the proposed nonlinear scaling methodology. Afterwards, results are analyzed, followed by a conclusion.

II. Operational Analysis and Design

The combined-excitation synchronous motor in its inner rotor (IR) configuration, with example solid model rendering shown in Fig. 1a and the CAD model of an experimentally validated prototype, which was tested up to a maximum power rating of 176kW, in Fig. 1b, has an active outer stator with tangentially magnetized PMs and toroidal AC coils working with a simple reluctance inner rotor. This configuration allows for flux intensification for high power density, reduced losses from shortened end turns, and high-speed high-efficiency operation as shown in Fig. 2 since the rotor has no active components amongst other benefits [13], [15], [23].

The machine operates based on the interaction of the stator fields, comprising the PM and armature fields, with the rotor reluctance. The number of pole pairs of the machine is determined by the number of rotor protrusions, with 14 being a typical selection for achieving high efficiency and high power density [13], [15]. The electromagnetic torque, T_e, can be obtained according to Maxwell's stress tensor method expressed by:

$$T_e = \frac{D_g^2 \ell_{stk}}{4\mu_0} \int_0^{2\pi} B_r B_t \, d\theta, \tag{1}$$

where D_g is the airgap diameter, ℓ_{stk} is the stack length, B_r and B_t are the radial and tangential components of the flux density B. In this machine topology, where T_e can be seen to ideally scale with ℓ_{stk} and the square of D_g. The presence of a ferrous core introduces nonlinearity, especially at high electrical loadings, which introduces additional complexity in the performance scaling of this machine. This behavior, which has been captured through simulation and experimentation by studying the torque and torque constants with increasing current density, is shown in Fig. 3.

Other very important performance metrics, such as the steady-state core loss, P_{Fe}, under the assumption that the dominant contribution comes largely from the fundamental frequency, f, can also be expressed as:

$$\begin{aligned} P_{Fe} = k_h f B^{\alpha} &+ \sum_{v=1}^{\infty} k_{ev} (vf)^2 \left(B_{r,v}^2 + B_{t,v}^2\right) \\ &+ \sum_{v=1}^{\infty} k_{av} (vf)^{1.5} \left(B_{r,v}^{1.5} + B_{t,v}^{1.5}\right) \end{aligned} \tag{2}$$

where v is the harmonic order [24]. This quantity is also highly nonlinear and difficult to scale with changing motor geometry and power ratings. Performance scaling in this machine is therefore a complex, highly nonlinear problem that may benefit from innovative approaches, as discussed in the subsequent sections of this paper.

III. DE and FEA for ML Training

An experimentally calibrated 14 rotor protrusion IR-PM motor parametric model was configured as shown in Fig. 4 and solved using the 2D Maxwell solver on Ansys Electronics Desktop [6]. The optimal selected ranges of its geometric vari-

ables, as detailed in Table I, were obtained through extensive sensitivity studies and design of experiments (DoE) to ensure realistic and mechanically stable designs are obtained in a DE process [25], [26].

The proposed novel method for nonlinear scaling, employing a hybrid DE and meta-modeling approach, is illustrated in the flowchart shown in Fig. 7. The DE process acts as the initial step, generating 2D FEA data for subsequent meta-modeling and scaling. Multi-objective DE using FEA is performed to *minimize* two concurrent objectives relating to the ratio of stack length to average torque, $\mathcal{F}_1$, and motor loss, $\mathcal{F}_2$:

$$\begin{aligned} \mathcal{F}_1 &= \frac{\ell_{stk}}{T_e}, \\ \mathcal{F}_2 &= P_{loss} = P_{Cu} + P_{Fe}, \end{aligned} \tag{3}$$

The objective function for motor loss, P_{loss}, was calculated as the sum of the variable and constant losses of the motor, where P_{Fe} represents the core loss (constant losses) and P_{Cu} represents the copper loss (variable losses) at a current density of 20A/mm^2 similar to the peak loading to the experimentally validated prototype. This was done to mimic a real-life situation and to reduce the impact of inherent nonlinearities and saturation effects on the scaling studies.

Two large FEA datasets are generated considering a fixed rated speed of 3,000rpm. The first dataset (DS1) consists of designs with a fixed stator outer diameter (OD) of 10″, all with an output power of 100 kW. The second dataset (DS2) includes designs at different power ratings of 50kW, 75kW, 100kW, 250kW, and 500 kW at individual fixed ODs of 7″, 8″, 10″, 12″, and 20″, respectively. A base airgap length of 0.5mm was multiplied by an airgap length multiplier factor, k_g, for each design according to their ODs, as shown in Fig. 5. This aligns with the expectation that a machine with a larger OD would typically have a larger airgap length, accounting for mechanical engineering considerations and constraints [11], [27].

In both cases, a two-tier analysis ensures each design meets the required torque for the specified power. Initially, torque is calculated using FEA, and then the stack length, ℓ_{stk}, is adjusted to achieve the specified rated torque for the power requirement. Once the torque requirement is satisfied, the evaluation of the objectives and other performance criteria proceeds.

IV. Meta-modeling and Nonlinear Scaling

Given the existing gap in literature concerning comprehensive methods for nonlinear scaling of special topology electric machines like the IR-PM, machine learning offers a promising approach for performance estimation and scaling through meta-modeling. As illustrated in Fig. 7, this inventive approach could reduce the computational effort in motor design while enabling performance estimation within acceptable tolerances for larger, higher-power motor designs using data derived from smaller, lower-power prototypes.

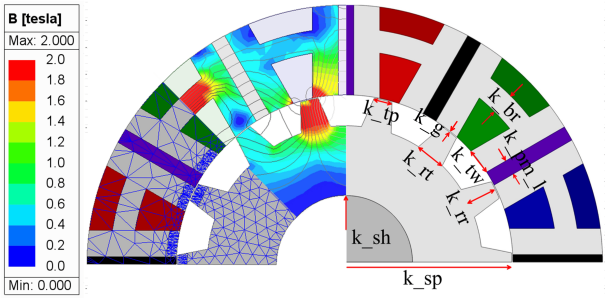

Fig. 4. Cross-sectional view of an IR-PM motor design with 8 labeled geometric independent variables considered in the multi-objective differential evolution.

Table I
Independent variables for the IR-PM differential evolution, and their ranges.

Variable	Description	Min	Max
k_sp	split ratio	0.60	0.70
k_pm_l	PM width ratio	10.00	20.00
k_br	bridge length ratio	0.17	0.33
k_tw	stator tooth width ratio	0.15	0.30
k_tp	rotor pole top ratio	0.40	0.80
k_rt	rotor pole root ratio	0.35	0.65
k_rr	rotor pole depth ratio	0.20	0.40
k_g	airgap length ratio	1	2
OD	stator OD [inches]	7	20

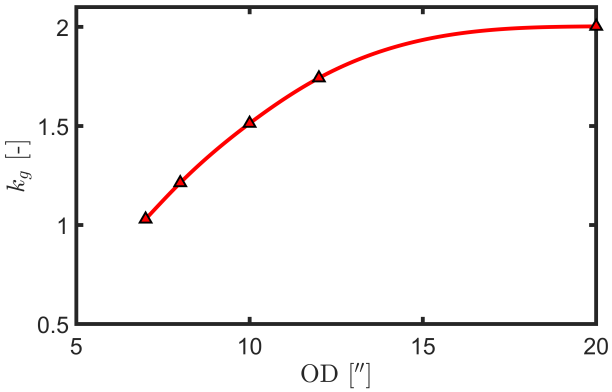

Fig. 5. A plot of the airgap length ratio k_g vs selected ODs for different power ratings considered for datasheet DS2 used for nonlinear scaling studies. In line with practical considerations, the airgap changes minimally at larger ODs.

Using TensorFlow [28], a similar artificial neural network (ANN) architecture as previously discussed was set up, having more advanced features to address the high nonlinearity in the data and nature of this study. Several advanced techniques were incorporated: Dropout was employed to prevent overfitting, while the Adam optimizer combined with ReduceLROnPlateau dynamically adjusted the learning rate to facilitate convergence and escape local minima. Additionally, L2 regularization was applied to discourage over-reliance on specific features, ensuring balanced model complexity. Batch normalization was implemented between layers to stabilize training and accelerate learning. The Swish activation function was chosen for its smooth gradient properties, enhancing the

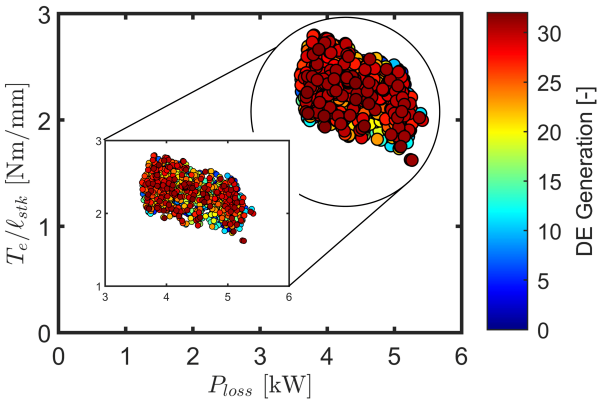

Fig. 6. Design data obtained using multi-objective differential evolution for a 100kW IR-PM topology for the ratio of average torque to stack length and motor loss objectives.

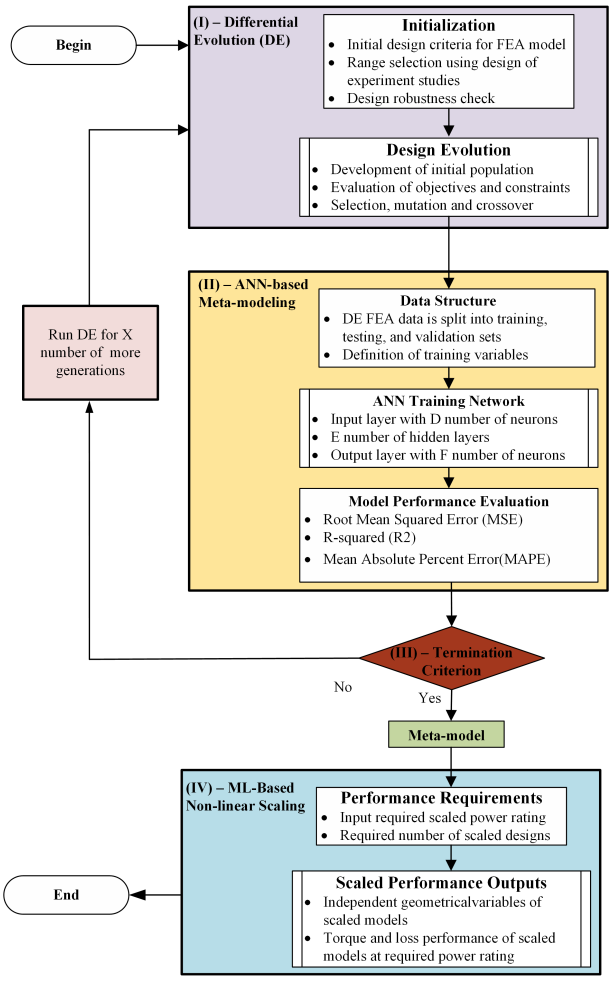

Fig. 7. A flowchart showing the stages in the novel ML-based nonlinear scaling approach for electric machines. Differential evolution (DE) serves as an input stage for generating data to train a satisfactory meta-model, which is thereafter used for nonlinear scaling at different power ratings.

network's ability to model complex relationships. A power-aware consideration was introduced to enhance generalization, ensuring that the model learned the ranges of typical per-

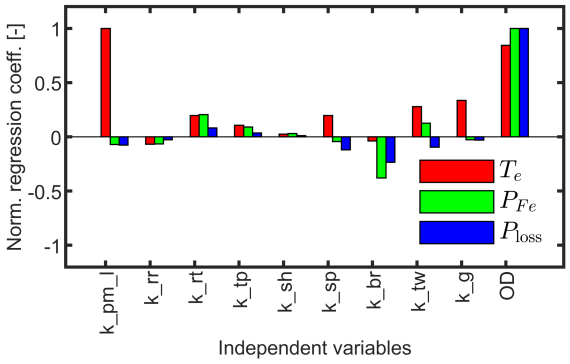

Fig. 8. Normalized nonlinear regression coefficients showing the influence of independent variables at peak loading and expected operating temperature on the average torque (T_e), core loss (P_{Fe}), and motor loss (P_{loss}).

formance values at different power ratings. This enables the model to further improve its prediction accuracy. Together, these techniques create a robust and efficient architecture, making it well-suited for regression tasks while prioritizing performance, generalization, and computational efficiency.

Two separate ANN models were trained on performance data of T_e/ℓ_{stk} and P_{Fe}, respectively. From the candidate designs, a random selection of 50% was employed for training, 30% for validation, and the remaining 20% for testing the ANN meta-model. The generalization capability of the ANN will be assessed by analyzing the error values for the training and validation datasets over 50 epochs. A termination criterion determines when the meta-model is considered satisfactory, which could include user-defined error values, model-determined generalization rate, elapsed time, the number of DE generations, or a combination of these factors. The total number of designs required for a particular power rating was considered as a termination factor in this study.

For nonlinear scaling studies, two example scenarios are considered using datasets DS1 and DS2 from the previous section. In case study 1 (CS1), which considers scaling at a fixed OD of 10″, DS1, which contains 1,300 designs as shown in Fig. 6, is used to train the meta-model. The ANN model for predicting the ratio T_e/ℓ_{stk} was trained using all 8 geometric input parameters described in Fig. 4, while the model for P_{Fe} included these same parameters along with ℓ_{stk} making 9 variables. Then, a nonlinear scaling from 50kW to 250kW is carried out. The performance of 50 designs for different power ratings in the range is predicted and compared with FEA results. The prediction error and its standard deviation trend are shown in Fig. 10.

For case study 2 (CS2), where OD and airgap length are allowed to vary, DS2 (6,500 designs) is used to train the meta-model. For this unique case, where the varying OD and airgap length introduce more nonlinearity compared to CS1, a reduced number of the most influential geometrical variables is used to enable better model training [26]. The OD is highly influential on torque and loss metrics, as demonstrated by the sensitivity analysis in Fig. 8. As such, only 6 variables are used to train the T_e/ℓ_{stk} model: OD, k_sp, k_pm_l, k_tw, k_rt,

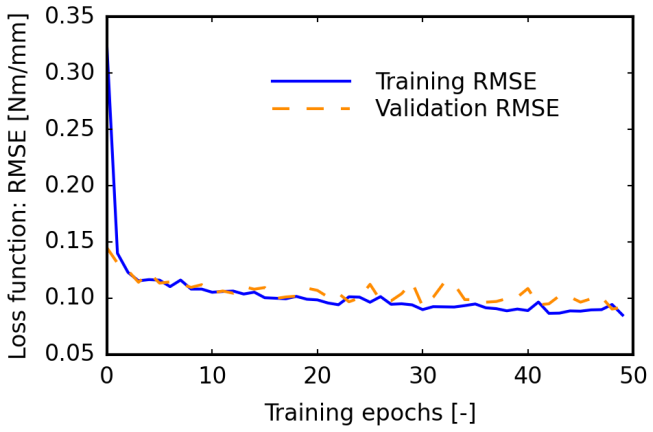

(a)

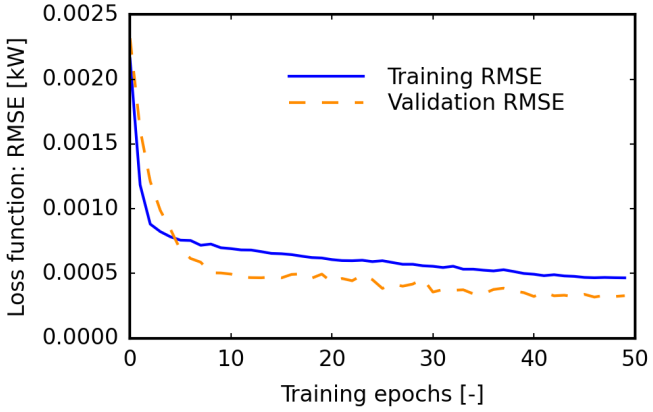

(b)

Fig. 9. The output trends for the ANN-based meta-modeling for CS1 showing the progression of the RMSE for the training and validation sets over all 50 epochs with a rapid decline during the first 10 epochs and stabilization afterward indicative of effective learning for (a) T_e/ℓ_{stk}, and (b) P_{Fe}.

and k_g. For the P_{Fe} model, an additional variable for ℓ_{stk} is included along with a consideration for power stratification for better generalized correlation of P_{Fe} values. Then, a nonlinear scaling for power ratings of 60, 90, 200, and 400kW at 7, 8, 11, and 15″ ODs, respectively, is performed by predicting the performance of 50 designs for each power rating. The prediction error and its standard deviation trend are shown in Fig. 11.

V. Results and Discussion

The ANN models showed good correlation between training and validation across the epochs as shown in Figs 9a and 9b. The performance of the ANN meta-models was evaluated using R-squared (R^2), and normalized root mean square error (NRMSE). The low values of error obtained validate the meta-model's ability to capture the nonlinear relationships in T_e/ℓ_{stk} and P_{Fe}.

The ANN meta-models for T_e/ℓ_{stk} and P_{Fe} demonstrated strong performance in both cases, with CS1 achieving an R-squared (R^2) of 0.9959 and an NRMSE of 1.22% for T_e/ℓ_{stk}, and an R^2 of 0.9885 with an NRMSE of 1.94% for P_{Fe}. In

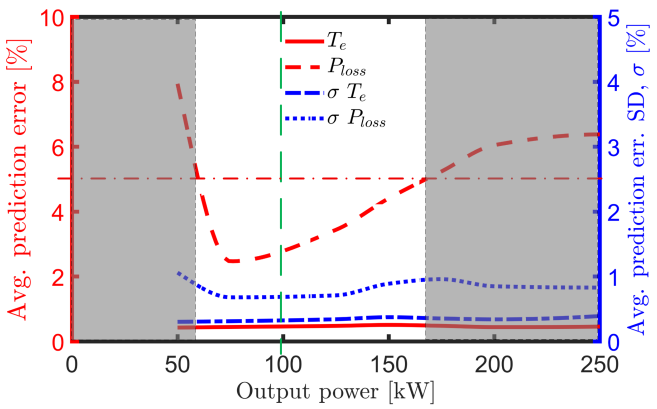

Fig. 10. Trend of absolute average prediction errors following nonlinear scaling using the ML meta-model developed in case study 1 (CS1). The vertical green dotted line denotes the power rating where ML training was done, and the gray areas have prediction errors above 5%.

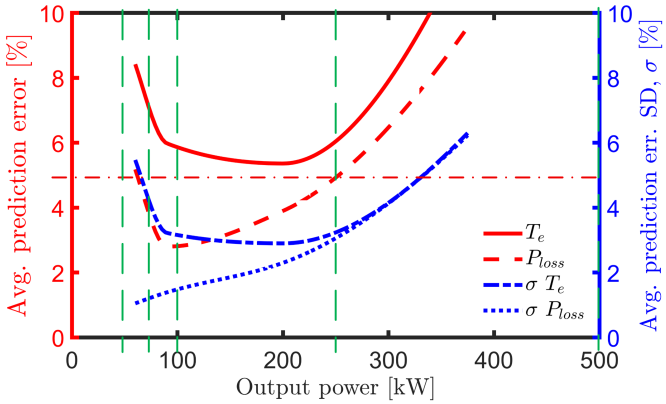

Fig. 11. Trend of absolute average prediction errors following nonlinear scaling using the ML meta-model developed in case study 2 (CS2). The vertical green dotted lines denote the power ratings where ML training was done.

CS2, the models performed even better for T_e/ℓ_{stk}, with an R^2 of 0.9994, while for P_{Fe}, the R^2 was 0.9492. This indicates substantial accuracy in the meta-model's ability to replicate the nonlinear patterns present in T_e/ℓ_{stk} and P_{Fe}.

The prediction error trends for CS1 and CS2 are captured in Figs. 10 and 11. Overall, the average prediction errors can be seen to be within a maximum tolerance of about 10% with low standard deviations. As expected, the errors are smallest when the predicted performance is close to the power rating area where training data was provided. This suggests that the closer the power ratings of the training sets, the lower the prediction errors for power ratings in between. The airgap is a geometrical nonlinearity, but also introduces a magnetic characteristic nonlinearity. This is evident in the generally higher error values seen in CS2 as compared to CS1. Overall, this shows that the proposed approach can be used for non-linear scaling and general performance estimation of highly nonlinear synchronous machines, with best performance in unsaturated low-speed operating conditions.

VI. Conclusion

A novel ML-based meta-modeling approach for the nonlinear scaling of electric machines is presented, addressing a critical gap in the literature. The method is successfully applied to the nonlinear performance scaling of a high-performance, high-power-density combined-excitation synchronous motor topology. A wide spectrum of power ratings, ranging from 50 kW to 500 kW, is considered.

The inherent highly nonlinear behavior of this motor topology is first investigated through simulation and experimentation. It is then demonstrated that a hybrid differential evolution (DE) and meta-modeling approach can effectively capture this behavior and scale the machine's performance across varying geometries and power ratings. The ML meta-models for torque-to-stack-length ratio (T_e/ℓ_{stk}) and core loss (P_{Fe}) exhibit high accuracy, with R^2 values close to 1. The variation in airgap at different power ratings was found to be not only a geometrical nonlinearity but also a source of magnetic characteristic nonlinearity, significantly impacting nonlinear performance scaling. Despite this, nonlinear scaling for torque and power losses was achieved within a maximum error of 10%, which may be considered acceptable for the broad range of power ratings examined.

Acknowledgment

The support of ANSYS Inc., and of University of Kentucky, the L. Stanley Pigman Chair in Power Endowment is gratefully acknowledged.

References

[1] J. Swanke, H. Zeng, D. Bobba, T. M. Jahns, and B. Sarlioglu, "Design and testing of a modular high-speed permanent-magnet machine for aerospace propulsion," in *2021 IEEE International Electric Machines & Drives Conference (IEMDC)*, 2021, pp. 1–8.

[2] B. Sarlioglu, C. T. Morris, D. Han, and S. Li, "Driving toward accessibility: A review of technological improvements for electric machines, power electronics, and batteries for electric and hybrid vehicles," *IEEE Industry Applications Magazine*, vol. 23, no. 1, pp. 14–25, 2017.

[3] I. Boldea, L. N. Tutelea, and A. A. Popa, "Reluctance synchronous and flux-modulation machines designs: Recent progress," *IEEE Journal of Emerging and Selected Topics in Power Electronics*, vol. 10, no. 2, pp. 1683–1702, 2022.

[4] B. Fahimi, L. H. Lewis, J. M. Miller, S. D. Pekarek, I. Boldea, B. Ozpineci, K. Hameyer, S. Schulz, A. Ghaderi, M. Popescu, B. Lehman, and D. D. Patel, "Automotive electric propulsion systems: A technology outlook," *IEEE Transactions on Transportation Electrification*, pp. 1–1, 2023.

[5] M. Gobbi, A. Sattar, R. Palazzetti, and G. Mastinu, "Traction motors for electric vehicles: Maximization of mechanical efficiency–a review," *Applied Energy*, vol. 357, p. 122496, 2024.

[6] *Ansys® Electronics, version 25.1, 2025, ANSYS Inc.*

[7] M. Rosu, P. Zhou, D. Lin, D. M. Ionel, M. Popescu, F. Blaabjerg, V. Rallabandi, and D. Staton, *Multiphysics simulation by design for electrical machines, power electronics and drives*. John Wiley & Sons, 2017.

[8] B. Praslicka, N. Taran, and C. Ma, "An ultra-fast method for analyzing ipm motors at multiple operating points using surrogate models," in *2022 IEEE Transportation Electrification Conference & Expo (ITEC)*, 2022, pp. 868–873.

[9] A. Allca-Pekarovic, P. J. Kollmeyer, A. Forsyth, and A. Emadi, "Experimental characterization and modeling of a YASA P400 axial flux PM traction machine for performance analysis of a chevy bolt EV," *IEEE Transactions on Industry Applications*, vol. 60, no. 2, pp. 3108–3119, 2024.

[10] M. Lehr, D. Dietz, and A. Binder, "Electromagnetic design of a permanent magnet flux-switching-machine as a direct-driven 3 MW wind power generator," in *2018 IEEE International Conference on Industrial Technology (ICIT)*, 2018, pp. 383–388.

[11] Y. Duan and D. M. Ionel, "Nonlinear scaling rules for brushless PM synchronous machines based on optimal design studies for a wide range of power ratings," *IEEE Transactions on Industry Applications*, vol. 50, no. 2, pp. 1044–1052, 2014.

[12] K. Ramakrishnan, S. Stipetic, M. Gobbi, and G. Mastinu, "Optimal sizing of traction motors using scalable electric machine model," *IEEE Transactions on Transportation Electrification*, vol. 4, no. 1, pp. 314–321, 2018.

[13] O. A. Badewa and D. M. Ionel, "Analysis and design of synchronous machines with reluctance rotor and PM stator combined excitation," in *2024 IEEE Energy Conversion Congress and Exposition (ECCE)*, 2024, pp. 1–6.

[14] A. Mohammadi, O. A. Badewa, Y. Chulaee, D. D. Lewis, S. Essakiappan, M. Manjrekar, and D. M. Ionel, "Design optimization of a direct-drive wind generator with a reluctance rotor and a flux intensifying stator using different PM types," *IEEE Transactions on Industry Applications*, pp. 1–10, 2024.

[15] O. A. Badewa, A. Mohammadi, D. D. Lewis, S. Essakiappan, M. Manjrekar, and D. M. Ionel, "Electromagnetic design characterization of synchronous machines with flux switching effect employing reluctance rotors and stators with PMs and AC concentrated coils," *IEEE Transactions on Industry Applications*, pp. 1–14, 2025.

[16] B. F. Azevedo, A. M. A. Rocha, and A. I. Pereira, "Hybrid approaches to optimization and machine learning methods: a systematic literature review," *Machine Learning*, pp. 1–43, 2024.

[17] D. Barri, F. Soresini, M. Gobbi, A. d. Gerlando, and G. Mastinu, "Optimal design of traction electric motors by a new adaptive pareto algorithm," *IEEE Transactions on Vehicular Technology*, pp. 1–17, 2025.

[18] P. Asef and C. Vagg, "A physics-informed bayesian optimization method for rapid development of electrical machines," *Scientific Reports*, vol. 14, no. 1, p. 4526, 2024.

[19] M. Cheng, X. Zhao, M. Dhimish, W. Qiu, and S. Niu, "A review of data-driven surrogate models for design optimization of electric motors," *IEEE Transactions on Transportation Electrification*, pp. 1–1, 2024.

[20] M. D. Silva and S. Eriksson, "Meta-models for torque optimization of spoke type permanent magnet synchronous machines," in *2023 24th International Conference on the Computation of Electromagnetic Fields (COMPUMAG)*, 2023, pp. 1–4.

[21] M. Omar, M. Bakr, and A. Emadi, "Switched reluctance motor design optimization: A framework for effective machine learning algorithm selection and evaluation," in *2024 IEEE Transportation Electrification Conference and Expo (ITEC)*, 2024, pp. 1–6.

[22] A.-C. Pop, Z. Cai, and J. J. C. Gyselinck, "Machine-learning aided multiobjective optimization of electric machines— geometric-feasibility and enhanced regression models," *IEEE Journal of Emerging and Selected Topics in Industrial Electronics*, vol. 4, no. 3, pp. 844–854, 2023.

[23] C. S. Goli, M. G. Kesgin, P. Han, D. M. Ionel, S. Essakiappan, J. Gafford, and M. D. Manjrekar, "Analysis and design of an electric machine employing a special stator with phase winding modules and PMs and a reluctance rotor," *IEEE Access*, vol. 12, pp. 9621–9631, 2024.

[24] D. Ionel, M. Popescu, S. Dellinger, T. Miller, R. Heideman, and M. McGilp, "On the variation with flux and frequency of the core loss coefficients in electrical machines," *IEEE Transactions on Industry Applications*, vol. 42, no. 3, pp. 658–667, 2006.

[25] R. Storn and K. Price, "Differential evolution–a simple and efficient heuristic for global optimization over continuous spaces," *Journal of global optimization*, vol. 11, pp. 341–359, 1997.

[26] P. Asef and A. Lapthorn, "Overview of sensitivity analysis methods capabilities for traction AC machines in electrified vehicles," *IEEE Access*, vol. 9, pp. 23 454–23 471, 2021.

[27] T. A. Lipo, *Introduction to AC machine design*. John Wiley & Sons, 2017.

[28] M. Abadi *et al.*, "TensorFlow: Large-scale machine learning on heterogeneous systems," 2015, software available from tensorflow.org. [Online]. Available: https://www.tensorflow.org/